Cell Death and Differentiation (2016) 23, 1941–1951
 1350-9047/16
www.nature.com/cdd

IL-12p40 impairs mesenchymal stem cell-mediated bone regeneration via CD4$^+$ T cells

Jiajia Xu[1], Yiyun Wang[1], Jing Li[1,2], Xudong Zhang[1], Yiyun Geng[1], Yan Huang[1], Kerong Dai*[,1,2] and Xiaoling Zhang*[,1,2]

Severe or prolonged inflammatory response caused by infection or biomaterials leads to delayed healing or bone repair failure. This study investigated the important roles of the proinflammatory cytokines of the interleukin-12 (IL-12) family, namely, IL-12 and IL-23, in the inflammation-mediated inhibition of bone formation *in vivo*. *IL-12p40*$^{-/-}$ mice lacking IL-12 and IL-23 exhibited enhanced bone formation. IL-12 and IL-23 indirectly inhibited bone marrow mesenchymal stem cell (BMMSC) differentiation by stimulating CD4$^+$ T cells to increase interferon γ (IFN-γ) and IL-17 levels. Mechanistically, IL-17 synergistically enhanced IFN-γ-induced BMMSC apoptosis. Moreover, INF-γ and IL-17 exerted proapoptotic effects by upregulating the expression levels of Fas and tumor necrosis factor-related apoptosis-inducing ligand (TRAIL), as well as by activating the caspase cascade in BMMSCs. *IL-12p40* depletion in mice could promote ectopic bone formation. Thus, IL-12p40 is an attractive therapeutic target to overcome the inflammation-mediated inhibition of bone formation *in vivo*.
Cell Death and Differentiation (2016) **23,** 1941–1951; doi:10.1038/cdd.2016.72; published online 29 July 2016

Approximately 7.9 million fractures occur in the United States each year. Although most heal normally, 5–20% of fractures result in delayed or impaired healing requiring therapeutic intervention.[1] Bone marrow mesenchymal stem cell (BMMSC)-based therapy is an attractive option for augmenting the fracture repair process and BMMSCs have been used for the treatment of fracture non-union in clinical studies,[2,3] because of their fast and easy purification, amplification, multipotent differentiation ability, and low immunogenicity.[4,5] However, 10–18% of fractures stayed non-union after stem cell therapy in early clinical reports.[6] Patients suffering from non-union must undergo a second surgery, which may increase the economic burden on families, prolong the pain, and impaired the quality of life and work.[7] Inflammation is an important regulator of bone regeneration.[8,9] Following fracture injury, there is an initial inflammatory response that has a crucial role in bone healing.[1,10] However, severe or prolonged inflammatory response leads to delayed healing or bone repair failure.[11] Recent studies have shown that proinflammatory cytokines can impair bone repair in local injury. Interleukin-1β (IL-1β) suppresses matrix mineralization and osteoblastic marker gene expression *in vitro*.[12] Tumor necrosis factor α (TNF-α) inhibits osteogenic differentiation[12] and reduces bone formation in nude mice.[13] IL-4 and interferon γ (IFN-γ) are also significantly antiosteogenic.[14] Moreover, IFN-γ and TNF-α synergistically induce BMMSC apoptosis and significantly inhibit bone formation *in vivo*.[13] Meanwhile, IL-17 stimulates the nuclear factor kappa B (NF-κB) signaling pathway and impairs the differentiation of BMMSCs.[15] Therefore, defining the crosstalk between proinflammatory cytokines and BMMSCs is an important goal of the newly emerging osteoimmunology field, and such insights may also be helpful for designing improved protocols for BMMSC-mediated bone repair and regeneration.

The combination of BMMSCs with a suitable scaffold is an effective approach in bone tissue engineering to treat and reconstruct large bone defects.[16] Materials implanted into a body initiate a host response, which leads to inflammation and foreign body reactions.[17] Given their individual differences, some patients exhibit severe immune responses that lead to bone regeneration failure. Understanding the inflammatory factors and signaling pathways that participate in the healing is highly significant for clinical treatments and for predicting the effects of restoration. T cells have an important role in fracture healing process.[18,19] Intravenous infusion of pan T cells or CD4$^+$ T cells blocks bone formation in nude mice.[13] IL-12 and IL-23 are proinflammatory cytokines of the IL-12 family that are secreted by dendritic cells and tissue-resident macrophages to facilitate T-cell differentiation. IL-12 and IL-23 share a common p40 subunit (encoded by the *IL-12p40* gene).

[1]The Key Laboratory of Stem Cell Biology, Institute of Health Sciences, Shanghai Institutes for Biological Sciences (SIBS), Chinese Academy of Sciences (CAS); University of Chinese Academy of Sciences and Shanghai Jiao Tong University School of Medicine (SJTUSM), Shanghai 200031, China and [2]Shanghai Key Laboratory of Orthopaedic Implant, Department of Orthopaedic Surgery, Shanghai Ninth People's Hospital, Shanghai Jiao Tong University School of Medicine (SJTUSM), Shanghai 200011, China

*Corresponding author: K Dai or X Zhang, The Key Laboratory of Stem Cell Biology, Institute of Health Sciences, Room 1230 (116 mail box), life science building Block A, 320 Yueyang Road, Shanghai 200031, China. Tel: +86 21 54923338; Fax: +86 21 54923338; E-mail: krdai@163.com or xlzhang@sibs.ac.cn

Abbreviations: ALP, alkaline phosphatase; BMD, bone mineral density; BMMSC, bone marrow mesenchymal stem cell; β-TCP, β-tricalcium phosphate; BV/TV, bone volume/tissue volume ratio; CCK-8, Cell Counting Kit-8; Col1, type I collagen; CTX-1, collagen type I cross-linked C-telopeptide; DR5, death receptor 5; FasL, Fas ligand; FBS, fetal bovine serum; H&E, hematoxylin and eosin; IFN-γ, interferon γ; IL-1β, interleukin-1β; IL-12, interleukin-12; IOD, integral optical density; MAR, mineral apposition rate; Micro-CT, micro-computed tomography; NF-κB, nuclear factor kappa B; OCN, osteocalcin; Osx, osterix; PMNs, polymorphonuclear neutrophils; RT-PCR, real-time PCR; Runx2, runt-related transcription factor 2; siRNA, small interfering RNA; Tb.Sp, trabecular spacing; Tb.Th, Trabecular thickness; Th1, T helper type 1; TNF-α, tumor necrosis factor α; TNFR1, tumor necrosis factor receptor 1; TRAIL, tumor necrosis factor-related apoptosis-inducing ligand; TUNEL, TdT-mediated UTP nick end labeling; WT, wild type

Received 15.3.16; revised 28.4.16; accepted 31.5.16; Edited by RA Knight; published online 29 July 2016?

IL-12p40 has an important role in the development and progression of inflammation, and it can directly induce the development of T cells and enhance the production of immune factors.[20–22] Thus, IL-12 and IL-23 may have key roles in the inflammation-mediated inhibition of bone formation. However, the roles of the two cytokines in BMMSC-based bone regeneration are still poorly understood.

In the present study, we showed that deletion of IL-12 and IL-23 increased bone formation and bone mass in *IL-12p40*$^{-/-}$ mice. However, IL-12 and IL-23 exerted no direct effects on osteogenic differentiation of BMMSCs *in vitro* and *in vivo*. We also demonstrated that IL-12 and IL-23 indirectly inhibited BMMSC osteogenesis via CD4$^+$ T cells. CD4$^+$ T cells under the stimulation of IL-12 or IL-23 increased the expression of INF-γ or IL-17. IL-17 synergistically enhanced IFN-γ-induced BMMSC apoptosis. This mechanism was mediated by the upregulation of Fas and tumor necrosis factor-related apoptosis-inducing ligand (TRAIL) signaling pathways in BMMSCs. Knockdown of Fas or TRAIL arrested the proapoptotic effects of INF-γ and IL-17. Similarly, blocking the caspase cascade could also partially rescued BMMSC apoptosis. Finally, ectopic bone formation was significantly increased in *IL-12p40*$^{-/-}$ mice. Thus, IL-12p40 is a potential therapeutic target for bone repair in clinical practice.

Results

IL-12 and IL-23 inhibit BMMSC-osteoblast differentiation and bone formation *in vivo*. Immune cells, especially T cells, reportedly have an important role in bone regeneration.[13] Trauma and biomaterials can cause local inflammation. Thus, implanting BMMSCs mixed with biomaterials into C57BL/6J mice leads to the accumulation of a large number of immune factors around the implants. Severe inflammatory response affects bone repair.[13] We used an ectopic bone formation assay in C57BL/6J mice to detect the expression of immune factors in the implants. β-Tricalcium phosphate (β-TCP) is similar to bone in chemical composition and physical characteristics. Therefore, it has been widely used in clinical orthopedic surgery for almost 40 years.[23,24] In this study, we used β-TCP as the scaffold. Initially, we found the expression of IL-12 and IL-23 in the BMMSC implants. Notably, the concentrations of IL-23 in the BMMSC implants were elevated at 7–21 days after BMMSC implantation in C57BL/6J mice (Figure 1a). To explore whether or not IL-12 and IL-23 influence bone formation *in vivo*, we used a mouse model with global deletion of *IL-12p40* (B6.129S1-*Il12b*^{tm1Jm}/J, *IL-12p40*$^{-/-}$). The knockout mice lacked both IL-12 and IL-23.[21] Micro-computed tomography (Micro-CT) analysis of the left distal femur metaphysis revealed that the bone mineral density (BMD) and the bone volume/tissue volume ratio (BV/TV) of the *IL-12p40*$^{-/-}$ mice were significantly higher than those of the wild-type (WT) mice (C57BL/6J) at 2 months of age (Figures 1b–d). Trabecular thickness (Tb.Th) was also higher in the *IL-12p40*$^{-/-}$ mice than in the WT mice (Figure 1e), whereas trabecular spacing (Tb.Sp) was lower in the former than in the latter (Figure 1f). Histologic analysis showed that the *IL-12p40*$^{-/-}$ mice had more trabecular bone than the WT mice as indicated by hematoxylin and eosin (H&E) staining (Figure 1g). In addition, histomorphometric analysis revealed more osteoblast surface (Figure 1h) and less osteoclast surface (Figure 1i) in the 2-month-old *IL-12p40*$^{-/-}$ mice than in the WT mice. We also assessed the serum osteocalcin (OCN) levels, a marker of bone formation, and found that serum OCN levels were significantly higher in the *IL-12p40*$^{-/-}$ mice than in the WT mice (Figure 1j). By contrast, the *IL-12p40*$^{-/-}$ mice had lower serum concentrations of collagen type I cross-linked C-telopeptide (CTX-1), a marker of bone resorption (Figure 1k). We performed dynamic histomorphometric analysis by using double calcein labeling to confirm further whether or not *IL-12p40*$^{-/-}$ mice display increased bone formation and found a 1.63-fold increase in the mineral apposition rate (MAR) of the *IL-12p40*$^{-/-}$ mice compared with that of the WT mice (Figure 1l). Thus, the *IL-12p40*$^{-/-}$ mice had increased bone formation and reduced bone resorption. These results suggest that IL-12 and IL-23 can inhibit BMMSC-osteoblast differentiation and bone formation *in vivo*.

CD4$^+$ T cells are needed for IL-12 and IL-23 to inhibit osteogenic differentiation of BMMSCs. The *IL-12p40*$^{-/-}$ mice exhibited increased bone mass and bone formation. Therefore, we speculated that IL-12 and IL-23 directly inhibit BMMSC osteogenesis. To confirm this hypothesis, we subcutaneously implanted BMMSCs and β-TCP in nude mice with hydrogels to release IL-12 and IL-23. However, IL-12 and IL-23 treatments exerted no direct inhibitory effects on bone formation *in vivo* compared with the control mice (Figures 2a and b).

Subsequently, we induced osteogenic differentiation of BMMSCs by culturing in osteogenic medium *in vitro* and adding different doses (10–200 ng/ml) of IL-12 and IL-23. Similarly, treatment with IL-12 or IL-23 alone exhibited no direct inhibitory effect on BMMSC osteogenesis (Figures 2c and e). Then, we detected the expression levels of three differentiation markers (alkaline phosphatase (ALP), runt-related transcription factor 2 (Runx2), and OCN). The results were consistent with those obtained after Alizarin Red S staining (Figures 2d and f). Furthermore, treatment with the combination of IL-12 and IL-23 did not inhibit osteogenic differentiation of BMMSCs. The Alizarin Red S staining and the expression levels of the differentiation markers showed no difference after treatment with IL-12 and IL-23 alone or in combination (Figures 2g and h). Taken together, these results collectively suggest that IL-12 and IL-23 do not directly influence osteogenic differentiation of BMMSCs.

These results prompted us to investigate whether or not IL-12 and IL-23 exert indirect effects on BMMSC differentiation. T cells have an important role in adaptive immunity, and naive T cells differentiate into T helper type 1 (Th1) and Th17 cells depending on IL-12 and IL-23,[25] respectively. IL-12 and IL-23 might indirectly inhibit osteogenic differentiation and bone formation because nude mice lack functioning T cells.[26] To confirm this hypothesis, we isolated mouse CD4$^+$ T cells and treated them with IL-12 and IL-23. Then, we collected the culture supernatants and induced osteogenic differentiation of BMMSCs by culturing in osteogenic medium plus the supernatants. Interestingly, the osteogenesis of BMMSCs was significantly inhibited by the IL-12- and IL-23-treated

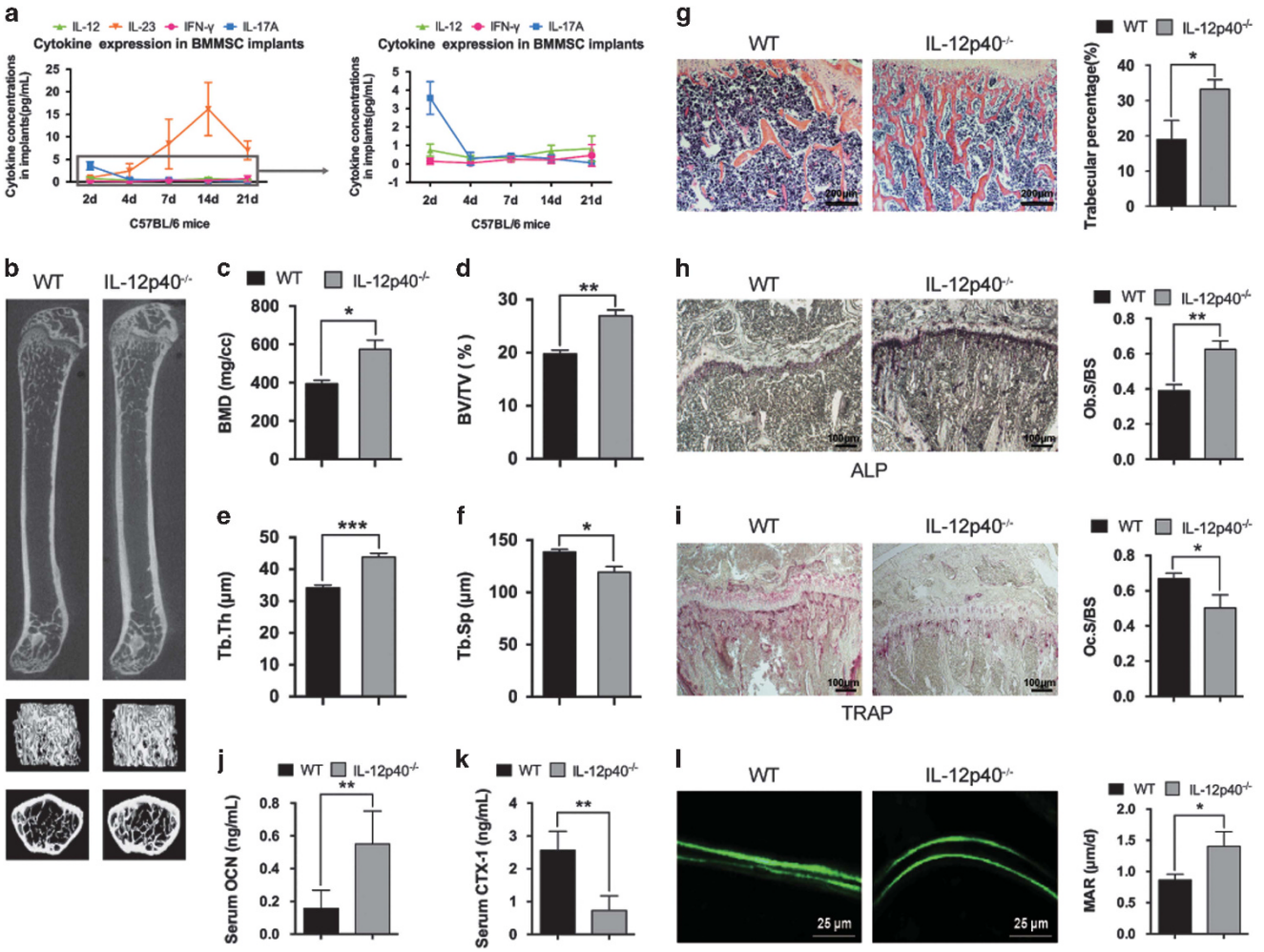

Figure 1 *IL-12p40*$^{-/-}$ mice increased bone formation and inhibited bone resorption. (**a**) Cytokine expression in different time periods after implantation in C57BL/6J mice. $n=5$ per group. (**b**) Increased cortical bone thickness and trabecular bone in micro-CT images of the distal femur of *IL-12p40*$^{-/-}$ mice compared with WT mice. $n=5$ per group. (**c–f**) BMD (**c**), BV/TV (**d**), Tb.Th (**e**), and Tb.Sp (**f**) as measured by micro-CT. $n=5$ per group. (**g**) H&E staining of femur sections from 8-week-old WT and *IL-12p40*$^{-/-}$ mice. $n=5$ per group. Scale bars, 200 μm. (**h**) ALP staining and quantitative analysis by ImageJ showed a more osteoblast surface in the *IL-12p40*$^{-/-}$ mice compared with the WT mice. $n=5$ per group. Scale bars, 100 μm. (**i**) TRAP staining and quantitative analysis by ImageJ showed that osteoclast surface was reduced in the *IL-12p40*$^{-/-}$ mice compared with the WT mice. $n=5$ per group. Scale bars, 100 μm. (**j** and **k**) ELISA of serum concentrations of OCN (**j**) and CTX-1 (**k**) in 8-week-old WT *versus* *IL-12p40*$^{-/-}$ mice. $n=5$–8 per group. (**l**) Representative images (left) of new bone formation and quantification of the MAR (right) as assessed by double calcein labeling. $n=5$ per group. Scale bars, 25 μm. All values are given as the mean ± S.D. of three independent experiments. $^{*}P<0.05$, $^{**}P<0.01$, $^{***}P<0.001$

supernatants compared with the untreated supernatants (Figure 2i). Altogether, IL-12 and IL-23 do not directly inhibit BMMSCs differentiation, but they influence CD4^{+} T cells and indirectly inhibit osteogenic differentiation of BMMSCs.

IL-12 and IL-23 indirectly inhibit BMMSC differentiation by increasing IFN-γ and IL-17. To search for a mechanism that could explain the inhibitory effects of culture supernatants on BMMSC differentiation, we hypothesized that some cytokines are produced by CD4^{+} T cells after stimulation with IL-12 and IL-23. To test this hypothesis, we stimulated the CD4^{+} T cells with IL-12 or IL-23 and then analyzed the mRNA expression of T cell-derived cytokines via real-time PCR (RT-PCR). Among the tested cytokines, only IFN-γ was significantly upregulated after stimulation with IL-12 (Figure 3a and Supplementary Figure S1a). Similarly, only IL-17 was increased after stimulation with IL-23 (Figure 3a and Supplementary Figure S1b).

IL-12 induces IFN-γ production.[27] IL-23, a member of the IL-12 family, is an important cytokine for the differentiation of Th17 cells that produce IL-17.[27–29] Thus, we suspected that IL-12 and IL-23 inhibit the osteogenesis of BMMSCs through IFN-γ and IL-17. Compared with the WT mice, the *IL-12p40*$^{-/-}$ mice had lower serum levels of IFN-γ and IL-17 after implantation (Figure 3b). The cytokines were added in different concentrations (10–200 ng/ml) during *in vitro* osteogenesis to assess further the role of IFN-γ or IL-17 in BMMSC osteogenesis. We observed that the BMMSCs treated with IL-17 exhibited reduced osteogenesis at high concentrations, as indicated by Alizarin Red S staining (Figure 3c). As expected, gene expression analysis revealed downregulated expression of the three differentiation markers osterix (Osx), OCN, and

type I collagen (Col1) (Figure 3d). Furthermore, Alizarin Red S staining revealed that IFN-γ treatment inhibited osteogenesis in a dose-dependent manner (Figure 3e). The expression levels of differentiation markers (Osx, OCN, and Col1) were also significantly reduced (Figure 3f). The inhibitory effect of IFN-γ on osteoblast differentiation was stronger than those of

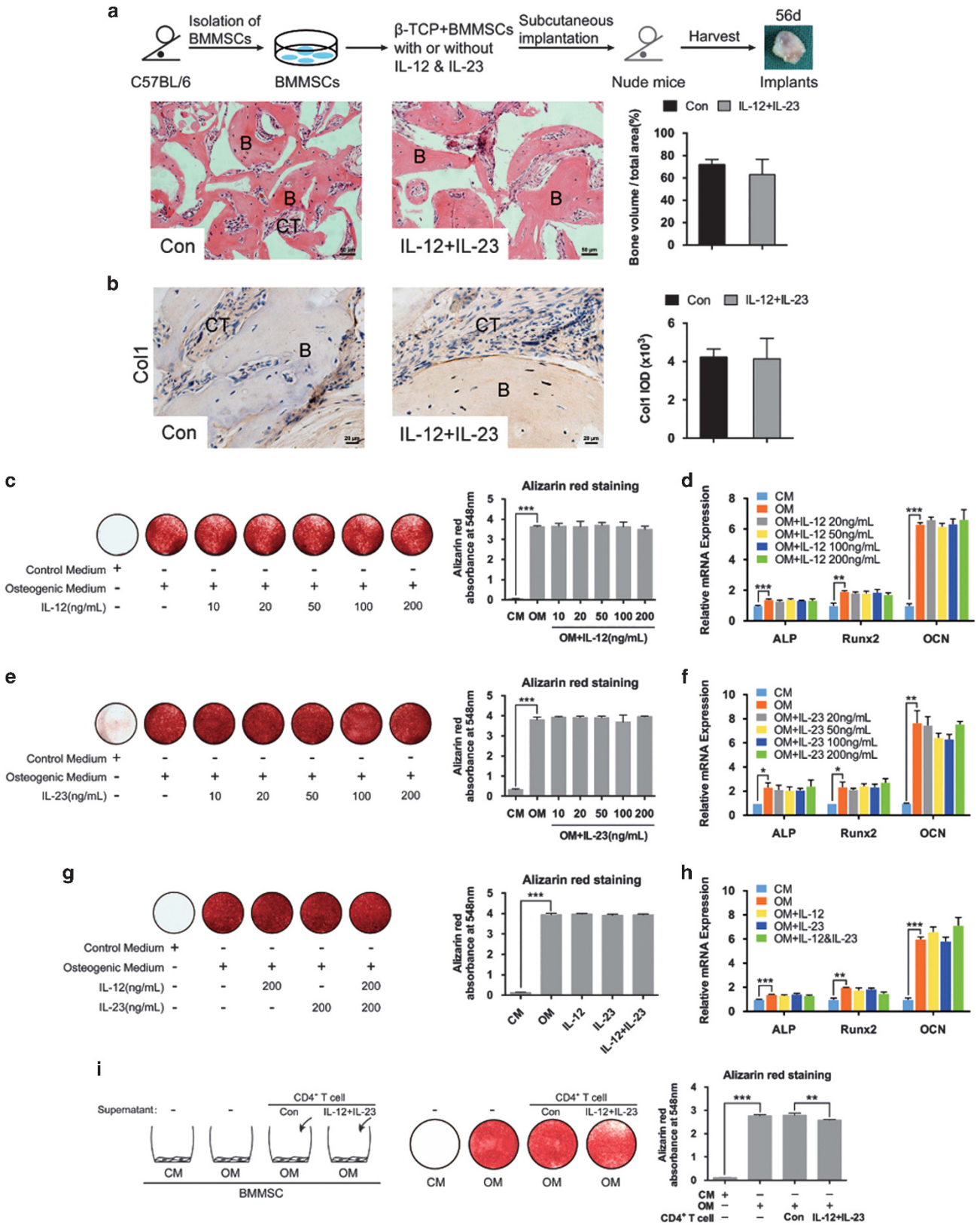

IL-17 at the same concentration. Moreover, the combination of IFN-γ and IL-17 displayed stronger inhibition of osteogenesis compared with that of either cytokine alone, especially at high concentration levels (200 ng/ml) (Figures 3g and h). Therefore, we treated BMMSCs with 200 ng/ml IFN-γ and 200 ng/ml IL-17 in all subsequent experiments. IL-17 slightly inhibited osteogenic differentiation, whereas IFN-γ strongly inhibited the expression of Runx2, ALP, Osx, OCN, and Col1. However, IL-17 could markedly amplify the inhibitory effect of INF-γ on osteogenesis (Figures 3i and j). Taken together, these observations strongly suggest that IL-12 and IL-23 indirectly inhibit BMMSC osteogenic differentiation by increasing the expression of INF-γ and IL-17.

IL-17 synergistically enhances BMMSC apoptosis induced by IFN-γ. We learned that IL-17 significantly enhanced the inhibitory effect of INF-γ on osteogenesis. Therefore, we speculated that IFN-γ and IL-17 exert an additive effect on the osteoblast differentiation of BMMSCs. We first detected IFN-γ- and IL-17-related pathways and found that IL-17 activated the NF-κB (p65) and MAPK (p38 and JNK) pathways and that STAT1 was phosphorylated in response to IFN-γ (Figure 4a). The combination of IFN-γ and IL-17 stimulation did not enhance the above-mentioned signaling pathways. By contrast, the p65, p38, and JNK signaling pathways were weakened compared with BMMSCs stimulated by IL-17 alone (Figure 4a). Therefore, the effects of the combination of IFN-γ and IL-17 were not simply additive, and these data prompted us to examine other signaling pathways. IFN-γ reportedly induces apoptosis.[30,31] When we cultured BMMSCs with IL-17 or IFN-γ, IL-17 exerted no effect on cell death, but IFN-γ significantly induced BMMSC death in a dose-dependent manner. IFN-γ further caused BMMSC death in the presence of IL-17 (Figure 4b). To determine the effect of IL-17 on IFN-γ-induced cell death, we added 200 ng/ml IL-17 to BMMSCs that were treated with different doses of IFN-γ (ranging from 10 to 200 ng/ml). When IL-17 was added, only 10 ng/ml IFN-γ significantly enhanced BMMSC death (Figure 4c). To confirm further the synergistic effects of IFN-γ and IL-17, we added 200 ng/ml IFN-γ to BMMSCs with 10–200 ng/ml IL-17. As expected, the elevated levels of IL-17 gradually increased BMMSC death when combined with IFN-γ (Figure 4d). When the IL-17 concentration reached 200 ng/ml, the maximum number of BMMSCs killed was achieved (Figure 4d). These data indicate that IL-17 can synergistically promote BMMSC death induced by IFN-γ.

We first added IFN-γ and IL-17 to BMMSCs and detected the expression of the Fas/Fas ligand (FasL), TNF-α/tumor necrosis factor receptor 1 (TNFR1), and TRAIL/death receptor 5 (DR5) at different time points to determine whether or not cells died by apoptosis. IL-17 did not increase the expression of Fas and TRAIL, whereas TRAIL expression was strongly induced in BMMSCs upon IFN-γ stimulation. However, the combination of IFN-γ and IL-17 further upregulated Fas and TRAIL expression in BMMSCs (Figures 4e and f). In addition, western blot analysis showed that the combination of IFN-γ and IL-17 enhanced the activation of caspase 8 and caspase 3 (Figure 4g). Then, we used TdT-mediated UTP nick end labeling (TUNEL) staining to detect apoptotic cells. IL-17 alone exerted no effect on apoptosis, whereas IFN-γ induced BMMSC apoptosis. Furthermore, the combination of IFN-γ and IL-17 had a higher apoptotic rate and a lower percentage of surviving cells than either cytokine alone (Figures 4h–j). We immunostained cleaved caspase 3 in the implants to confirm further the apoptosis induced by IFN-γ and IL-17 *in vivo*. Results revealed that caspase 3 activity decreased in the *IL-12p40*$^{-/-}$ mice (Figure 4k). Consistent with activated caspase 3 staining, we found that TUNEL staining was also potently reduced in the *IL-12p40*$^{-/-}$ mice (Figure 4l). These results indicate that IL-17 can synergistically enhance IFN-γ-induced BMMSC apoptosis *in vitro* and *in vivo*.

Suppression of caspase activation can partially rescue osteogenic differentiation of BMMSCs. We used small interfering RNA (siRNA) and caspase inhibitors to block apoptosis to test whether or not inhibiting the apoptotic pathways could rescue the effects of IFN-γ and IL-17 on BMMSC differentiation. First, we designed siRNA to inhibit Fas and TRAIL expression in BMMSCs (Figures 5a and b). Knockdown of Fas or TRAIL expression in BMMSCs could block the activation of caspase 8 and caspase 3 when treated with IFN-γ alone or the combination of IFN-γ and IL-17 (Figure 5c). Blockage of Fas or TRAIL expression significantly inhibited BMMSC apoptosis (Figure 5d). Taken together, these results collectively suggest that the Fas and TRAIL signaling pathways are important in the BMMSC apoptosis induced by IFN-γ and IL-17. Furthermore, the reduction of Fas or TRAIL could rescue osteogenic differentiation inhibited by IFN-γ and IL-17 (Figure 5e). Then, we found that the inhibition of caspase activity with a caspase 3 inhibitor (Z-DEVD-FMK) or a pan-caspase inhibitor (Z-VAD-FMK) could reduce the number of apoptotic cells (Figure 5f). Moreover, blocking the caspase activity partially rescued IFN-γ- and IL-17-inhibited BMMSC osteogenesis (Figure 5g). In summary, these observations suggest that inhibiting the apoptotic pathways can partially rescue the effects of IFN-γ and IL-17 on BMMSC differentiation.

Figure 2 IL-12 and IL-23 indirectly inhibited osteogenic differentiation of BMMSCs. (**a**) Schema of the experimental procedures. New bone formation in nude mice was detected with H&E staining after implantation of BMMSCs and β-TCP plus IL-12 and IL-23 or no cytokine (control). Con, control; B, bone; CT, connective tissue. $n=5$ per group. Scale bars, 50 μm. (**b**) The Col1 expression levels of implants plus IL-12 and IL-23 or no cytokine in nude mice were shown by immunohistochemistry. $n=5$ per group. Scale bars, 20 μm. (**c** and **e**) Alizarin Red S staining of cultured BMMSCs after treatment with osteogenic medium plus different concentrations of IL-12 (**c**) or IL-23 (**e**). CM, control medium; OM, osteogenic medium. (**d** and **f**) Relative expression levels of osteoblast markers in BMMSCs indicated in (**c** and **e**) were quantified by RT-PCR. (**g**) Alizarin Red S staining of cultured BMMSCs after treatment with osteogenic medium plus IL-12 (200 ng/ml), IL-23 (200 ng/ml), or both. (**h**) Relative expression levels of osteoblast markers in BMMSCs indicated in (**g**) were quantified by RT-PCR. (**i**) Alizarin Red S staining of cultured BMMSCs after treatment with osteogenic medium plus supernatants of CD4$^+$ T cells that were stimulated with IL-12 and IL-23 or none (control). The relative levels of mRNA expression were normalized to β-actin. All values are given as the mean $\pm$ S.D. of three independent experiments. $^*P<0.05$, $^{**}P<0.01$, $^{***}P<0.001$

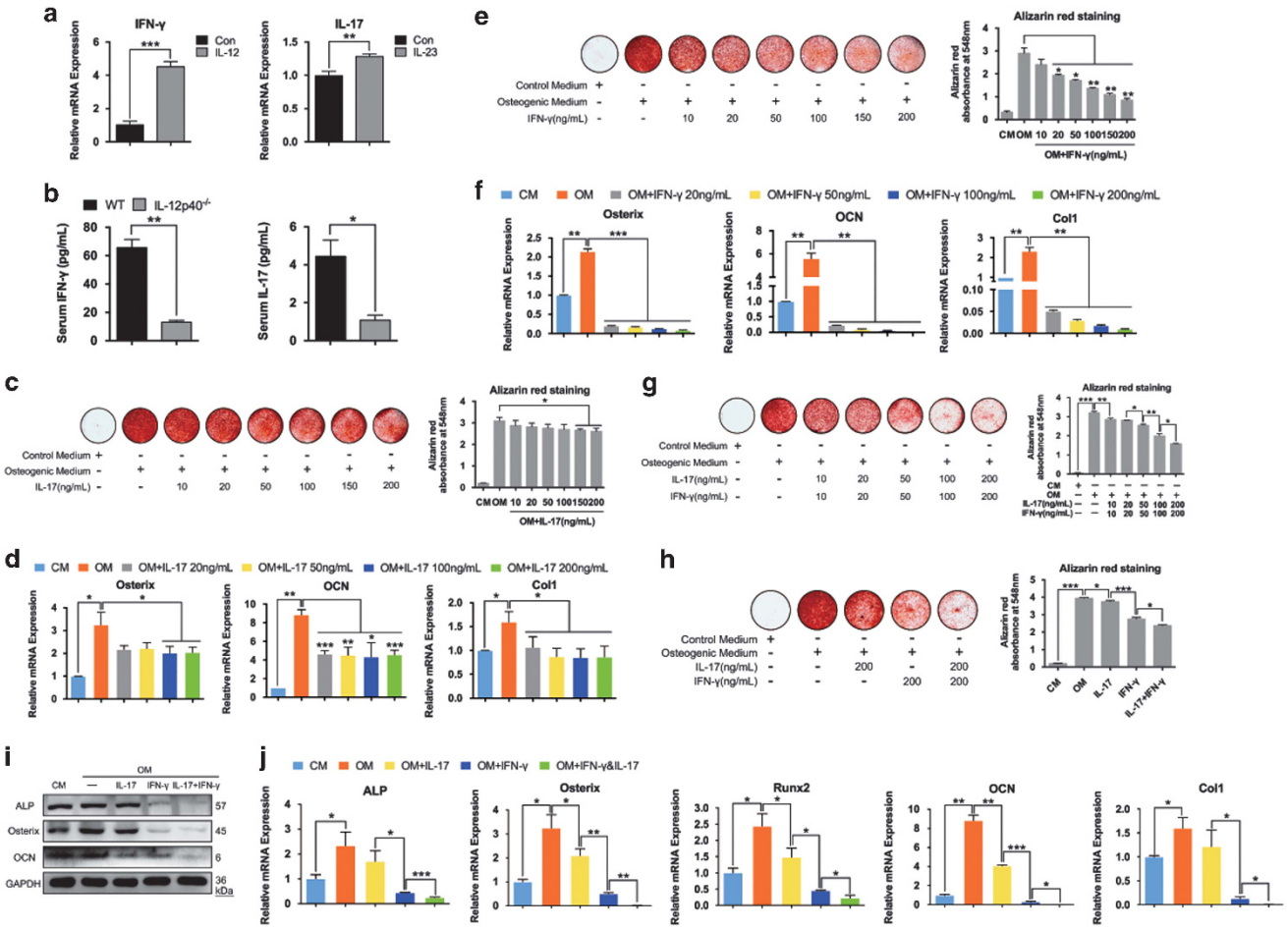

Figure 3 IL-12 and IL-23 upregulated IFN-γ and IL-17 to suppress BMMSC differentiation. (**a**) Expression of IFN-γ or IL-17 in CD4$^+$ T cells stimulated with IL-12 (200 ng/ml) or IL-23 (200 ng/ml). (**b**) Concentrations of serum IFN-γ and IL-17 after implantation in WT and *IL-12p40*$^{-/-}$ mice. (**c**, **e**, **g**, and **h**) Alizarin Red S staining of cultured BMMSCs after treatment with osteogenic medium plus different concentrations of IL-17 (**c**), IFN-γ (**e**), or both (**g** and **h**). (**d** and **f**) Relative expression levels of osteoblast markers indicated in (**c** and **e**) were quantified by RT-PCR. (**i**) Western blot analysis of the groups indicated in (**h**). (**j**) Relative expression levels of osteoblast markers in BMMSCs indicated in (**h**) were quantified by RT-PCR. The relative levels of mRNA expression were normalized to β-actin. All values are given as the mean $\pm$ S.D. of three independent experiments. $^*P<0.05$, $^{**}P<0.01$, $^{***}P<0.001$

IL-12p40 can act as a promising therapeutic target to promote BMMSC-mediated bone formation. The above results suggest that IL-12 and IL-23 inhibited BMMSC differentiation by upregulating IFN-γ and IL-17. Depletion of IL-12 and IL-23 *in vivo* would increase bone mass. The next question we wondered was whether depletion of IL-12 and IL-23 could promote BMMSC-mediated bone formation *in vivo*. In an attempt to solve this question, we combined BMMSCs with β-TCP graft and subcutaneously implanted these into WT or *IL-12p40*$^{-/-}$ mice. After 8 weeks, the implants were harvested (Figure 6a). Histologic analysis showed more bone formation in the *IL-12p40*$^{-/-}$ mice than in the WT mice (Figures 6b and c). An immunohistochemical analysis confirmed that the depletion of IL-12 and IL-23 promoted bone formation, as shown by the marked increase in the number of Col1-positive cells in the implants of *IL-12p40*$^{-/-}$ mice (Figures 6d and e). Therefore, these findings indicate that IL-12 and IL-23 have important roles in BMMSC-mediated bone formation *in vivo*. The two cytokines can delay bone formation and impair bone healing, but the reduction of IL-12 and IL-23 can promote bone repair *in vivo*.

Discussion

Fracture healing can be usually divided into three overlapping phases, namely, inflammation, repair, and remodeling.[18] The early inflammatory events following fracture are critical to the final outcome of fracture healing. Immune cells are a rich source of numerous cytokines that can affect the fate of bone cells during bone remodeling and disease. However, only a limited number of studies have focused on the relationship between the immune microenvironment and bone formation. In this study, we found that the levels of IL-12 and IL-23 in the implants were higher than those of other cytokines. As IL-12 and IL-23 share the p40 subunit, we then used a mouse model with global deletion of *IL-12p40* and found that *IL-12p40*$^{-/-}$ mice stimulated bone formation and increased bone mass. Therefore, these data supported our hypothesis that IL-12 and IL-23 have important roles in bone formation *in vivo*.

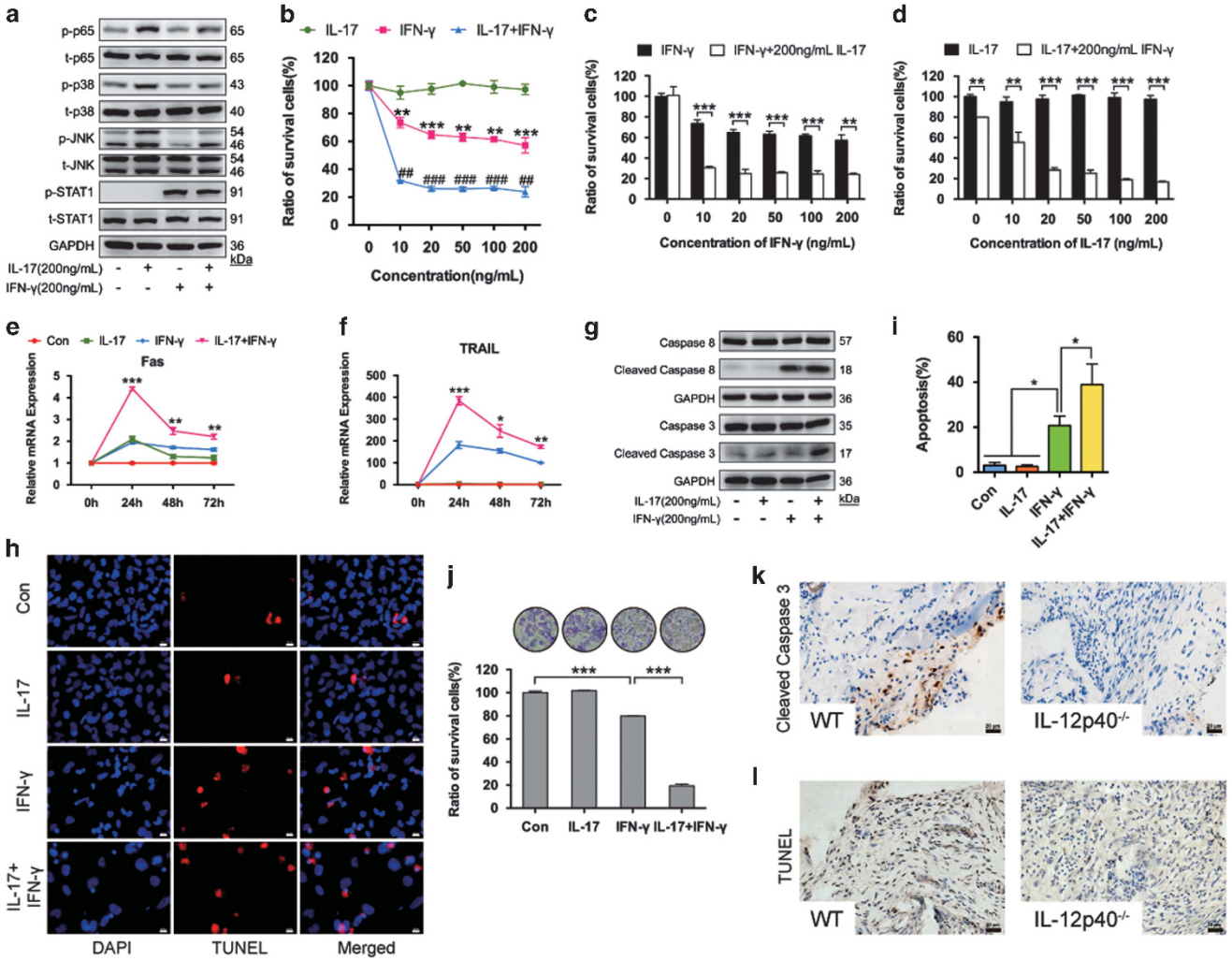

Figure 4 IL-17 synergistically promoted IFN-γ-induced BMMSC apoptosis *in vitro* and *in vivo*. (**a**) Western blot analysis of BMMSCs treated with IL-17 (200 ng/ml), IFN-γ (200 ng/ml), or both. (**b**) Percentage of surviving BMMSCs after treatment with different concentrations of IL-17, IFN-γ, or both. $^{**}P<0.01$, $^{***}P<0.001$ (*versus* IFN-γ/IL-17). $^{\#\#}P<0.01$, $^{\#\#\#}P<0.001$ (*versus* IFN-γ/IFN-γ+IL-17). (**c**) Ratio of surviving BMMSCs after treatment with various concentrations of IFN-γ (10–200 ng/ml) alone or in combination with IL-17 (200 ng/ml). (**d**) Ratio of surviving BMMSCs after treatment with various concentrations of IL-17 (10–200 ng/ml) alone or in combination with IFN-γ (200 ng/ml). (**e** and **f**) Relative expression levels of Fas (**e**) or TRAIL (**f**) in BMMSCs treated with IL-17 (200 ng/ml), IFN-γ (200 ng/ml), or both were quantified by RT-PCR. $^{*}P<0.05$, $^{**}P<0.01$, $^{***}P<0.001$ (*versus* IFN-γ/IFN-γ+IL-17). (**g**) Western blot analysis of cleaved caspase expression in BMMSCs after treatment with IL-17 (200 ng/ml), IFN-γ (200 ng/ml), or both. (**h**) Apoptosis of BMMSCs after treatment with IL-17 (200 ng/ml), IFN-γ (200 ng/ml), or both was detected by TUNEL staining. (**i**) Quantitative analysis of the apoptosis cells indicated in (**h**). (**j**) Cell apoptosis of BMMSCs after treatment with IL-17 (200 ng/ml), IFN-γ (200 ng/ml), or both, as demonstrated by toluidine blue staining. (**k** and **l**) The cleaved caspase 3 (**k**) and TUNEL (**l**) expression levels of implants in WT and *IL-12p40*$^{-/-}$ mice were shown by immunohistochemistry. $n=4$ per group. Scale bars, 20 μm. The relative levels of mRNA expression were normalized to β-actin. All values are given as the mean $\pm$ S.D. of three independent experiments. $^{*}P<0.05$, $^{**}P<0.01$, $^{***}P<0.001$

Further studies are needed to determine whether or not IL-12 and IL-23 impair BMMSC-mediated bone regeneration. Surprisingly, when we subcutaneously implanted BMMSCs and β-TCP in nude mice with IL-12 and IL-23, our results indicated that these two cytokines treatments exerted no direct inhibitory effects on bone formation *in vivo*. Nude mice are T-cell deficient.[26] T cells, especially CD4$^+$ T cells, have an important role in bone regeneration and fracture healing. Thus, we hypothesized that there is no direct inhibitory effects of IL-12 and IL-23 on bone formation because of the lack of mature T cells in nude mice. To test our hypothesis, we separated CD4$^+$ T cells and stimulated them with IL-12 and IL-23. Subsequently, we induced osteogenic differentiation of BMMSCs with the supernatant from CD4$^+$ T cells treated with IL-12 and IL-23. Obviously, the osteogenesis of BMMSCs was significantly inhibited, suggesting that CD4$^+$ T cells were needed for IL-12 and IL-23 to inhibit osteogenic differentiation of BMMSCs.

It is not known how CD4$^+$ T cells attribute to the IL-12 and IL-23-mediated blockage of osteogenic differentiation of BMMSCs. Hence, we stimulated the CD4$^+$ T cells with IL-12 or IL-23 and analyzed the mRNA expression of T cell-derived cytokines. Notably, IFN-γ and IL-17 were significantly upregulated after stimulation with IL-12 and IL-23, respectively. Alizarin Red S staining revealed that IFN-γ or IL-17 treatment inhibited osteogenesis in a dose-dependent manner.

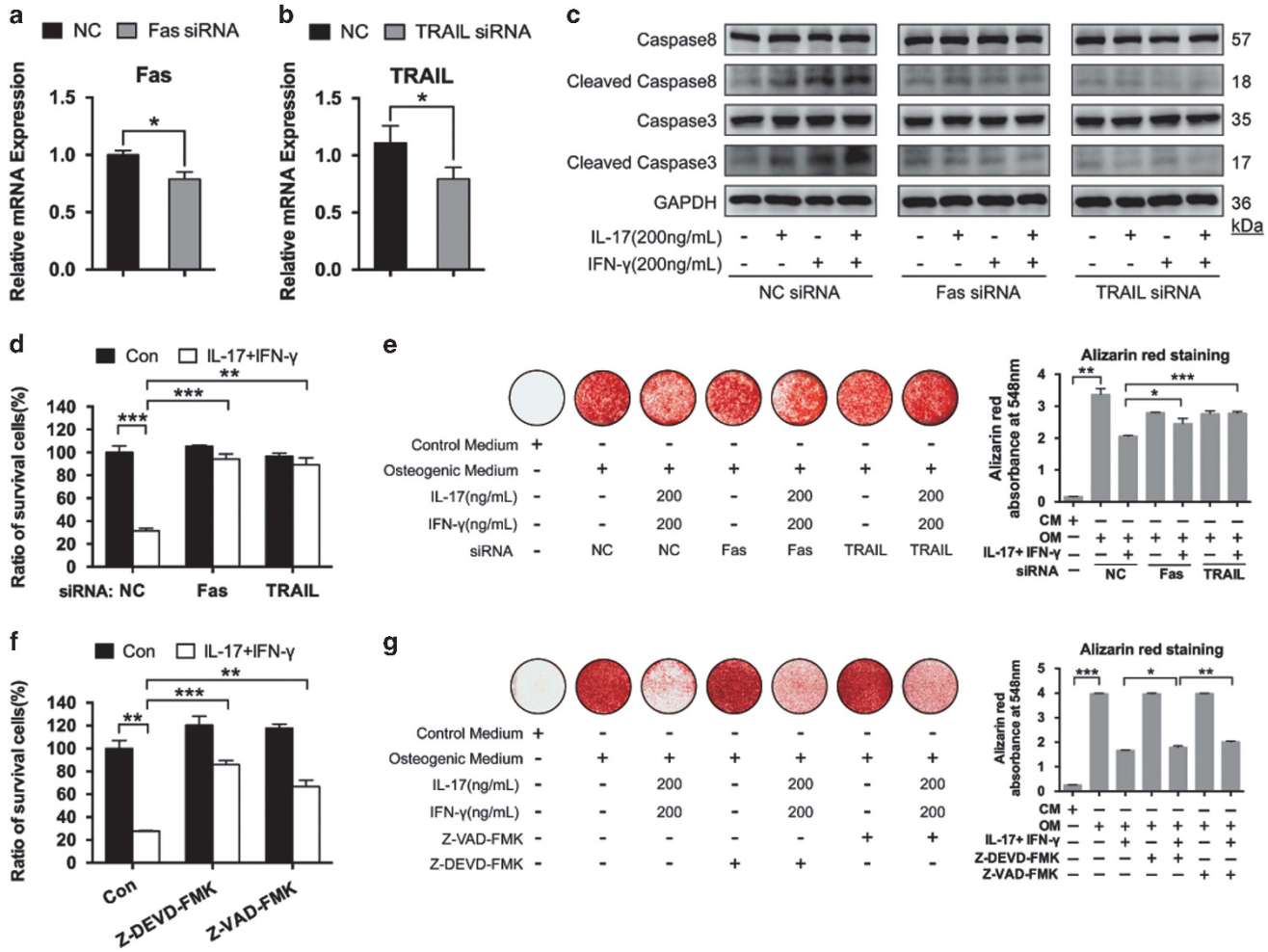

Figure 5 Inhibition of apoptosis could partially rescue osteogenic differentiation inhibited by IFN-γ and IL-17. (**a** and **b**) Knockdown of Fas (**a**) and TRAIL (**b**) expression by siRNA. NC, negative control. (**c**) Western blot analysis of cleaved caspase expression in BMMSCs after siRNA-mediated inhibition of Fas and TRAIL and treatment with IL-17 (200 ng/ml), IFN-γ (200 ng/ml), or both. (**d**) Ratio of surviving BMMSCs after siRNA-mediated inhibition of Fas and TRAIL and treatment with IL-17 (200 ng/ml) combined with IFN-γ (200 ng/ml). (**e**) Alizarin Red S staining of cultured BMMSCs after siRNA-mediated inhibition of Fas and TRAIL, and treatment with osteogenic medium alone or plus IL-17 (200 ng/ml) and IFN-γ (200 ng/ml). (**f**) Ratio of surviving BMMSCs after treatment with either a caspase 3 inhibitor (Z-DEVD-FMK) or a pan-caspase inhibitor (Z-VAD-FMK) alone or in combination with IL-17 (200 ng/ml) and IFN-γ (200 ng/ml). (**g**) Alizarin Red S staining of cultured BMMSCs after treatment with osteogenic medium and Z-DEVD-FMK or Z-VAD-FMK alone or in combination with IL-17 (200 ng/ml) and IFN-γ (200 ng/ml). The relative levels of mRNA expression were normalized to β-actin. All values are given as the mean $\pm$ S.D. of three independent experiments. $^*P<0.05$, $^{**}P<0.01$, $^{***}P<0.001$

Moreover, IL-17 could markedly amplify the inhibitory effect of IFN-γ on BMMSC osteogenesis. To further find out whether the inhibitory effects of IFN-γ and IL-17 are simply additive or other mechanisms, we detected IFN-γ- and IL-17-related signaling pathways. Our results showed that the combined effects of IFN-γ and IL-17 were not simply additive and IL-17-related signaling pathways displayed lower levels compared with IL-17 alone, indicating that IFN-γ and IL-17 suppressed osteogenic differentiation of BMMSCs by other mechanisms. Increasing evidence has shown that IFN-γ induces cell death.[32,33] Here, our results demonstrated that IFN-γ significantly increased BMMSC death in a dose-dependent manner. IFN-γ further caused BMMSC death in the presence of IL-17, suggesting that IL-17 synergistically promoted BMMSC death induced by IFN-γ. IFN-γ has also been shown to have a role in programmed cell death by increasing the expression of Fas/FasL and enhancing TRAIL-induced apoptosis.[34–36] Consistent with this, our study found that IFN-γ could induce BMMSC apoptosis. IL-17 synergistically enhanced IFN-γ-induced BMMSC apoptosis due to the upregulation of Fas and TRAIL expression levels in BMMSCs. Our *in vitro* and *in vivo* data indicated that the caspase cascade was activated and led to BMMSC apoptosis. In addition, our results also showed that blockage of apoptotic pathways partially rescued the inhibitory effects of IFN-γ and IL-17 on BMMSC differentiation.

Finally, we confirmed the possibility that IL-12p40 serves as a therapeutic target for inflammatory bone disorders. Strikingly, the formation of ectopic bone in the *IL-12p40*$^{-/-}$ mice was much more than that in the WT mice, suggesting its promising potential as a therapeutic target in clinical trials. IL-12p40 neutralizing antibodies have been used to treat various immune disorders, such as rheumatoid arthritis, psoriasis, psoriatic arthritis, and Crohn's disease.[37] In the

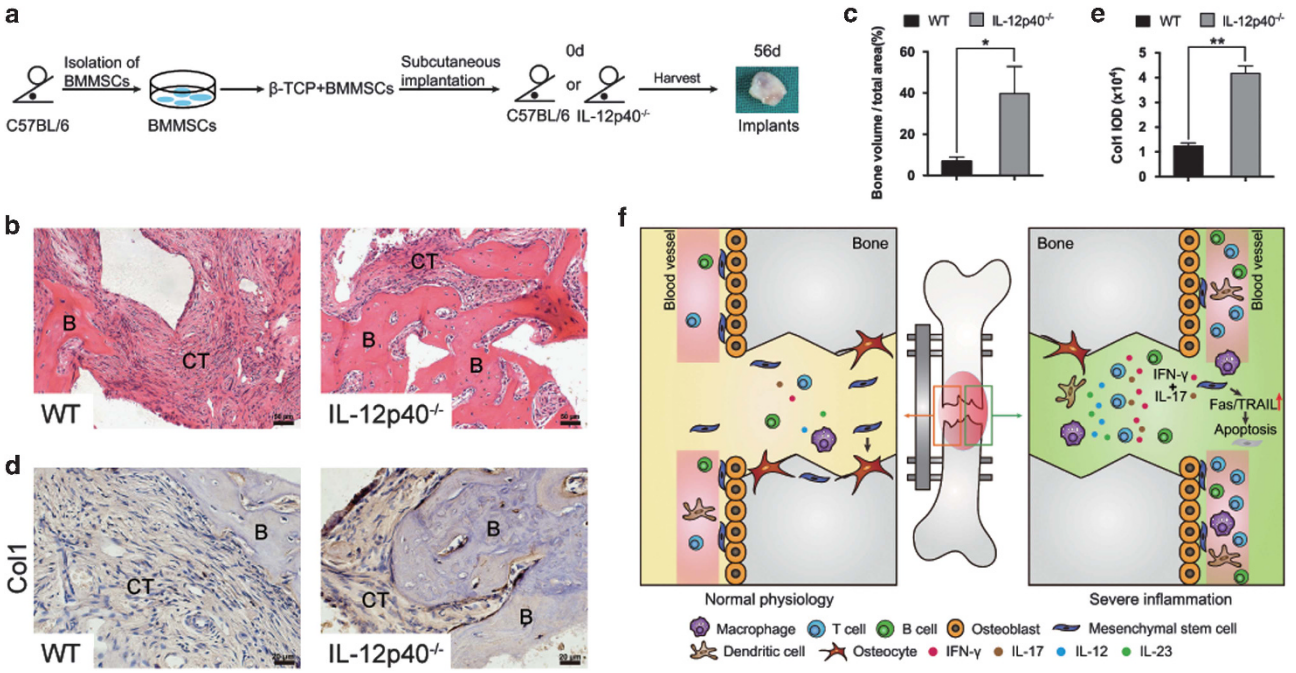

Figure 6 Depletion of *IL-12p40* promoted BMMSC-mediated bone formation. (**a**) Schema of the experimental procedures. BMMSCs mixed with β-TCP were subcutaneously implanted into the dorsal surface of WT or *IL-12p40*$^{-/-}$ mice. After 8 weeks, the implants were harvested. (**b**) New bone formation after implantation of BMMSCs and β-TCP in WT or *IL-12p40*$^{-/-}$ mice was detected with H&E staining. B, bone; CT, connective tissue. $n=5$ per group. Scale bars, 50 μm. (**c**) Quantitative analysis of new bone volume by ImageJ showed significantly increased new bone volume in *IL-12p40*$^{-/-}$ mice. $n=5$ per group. (**d**) Col1 expression levels of implants in WT or *IL-12p40*$^{-/-}$ mice were shown by immunohistochemistry. $n=5$ per group. Scale bars, 20 μm. (**e**) Quantification of Col1 expression in implants. $n=5$ per group. (**f**) Proposed role of IL-12 and IL-23 in fracture healing. With severe inflammation in the body, immune cells accumulate to the damaged tissue. These cells release large amounts of IL-12 and IL-23, which further promote the immune cells to produce other inflammatory factors (e.g., IFN-γ and IL-17). Locally produced IFN-γ and IL-17 can affect the function of BMMSCs and lead to BMMSC apoptosis. All values are given as the mean $\pm$ S.D. of three independent experiments. $^*P<0.05$, $^{**}P<0.01$

present paper, we showed that the expression levels of IL-12 and IL-23 were high in C57BL/6J mice and their presence could affect BMMSC-mediated bone regeneration. Depletion of *IL-12p40* in mice reduced the levels of IFN-γ and IL-17, and promoted bone regeneration *in vivo*. Therefore, treatment with neutralizing antibodies against IL-12p40 for bone regeneration may be a feasible and effective method. We expect that IL-12p40 will be developed as a biomarker for detecting bone repair and a therapeutic target for improving therapeutic outcome of BMMSC-based bone regeneration.

Under normal physiological conditions, fracture healing is initiated by inflammation, which can clear some cellular debris and bacteria *in vivo*. The appropriate inflammatory cytokines stimulate the differentiation of BMMSCs into osteoblasts. However, a large number of immune cells (resident macrophages, dendritic cells, T and B cells) accumulate to the damaged tissue when severe inflammation occurs in the body. These immune cells release large amounts of proinflammatory cytokines, such as IL-12 and IL-23. Proinflammatory cytokines of the IL-12 family can upregulate the levels of IFN-γ and IL-17 *in vivo*. Locally produced IFN-γ and IL-17 affect the function of BMMSCs and upregulate the expression of Fas and TRAIL in BMMSCs. Increased Fas and TRAIL expression activates the caspase cascade, leading to BMMSC apoptosis and impair bone regeneration (Figure 6f). Moreover, the inhibition of IL-12p40 can significantly promote bone repair, suggesting its promising potential as a therapeutic target. IL-12p40 antagonists may be an ideal and safe therapeutic agent for the inflammation-mediated inhibition of bone regeneration.

Materials and Methods

Mice. B6.129S1-*Il12b*^{tm1Jm}/J mice were purchased from Jackson Labs (Bar Harbor, ME, USA). Male C57BL/6J, immunocompromised nude mice (Balb/c, *nu/nu*) were purchased from Shanghai SLAC Laboratory Animal Co., Ltd (Shanghai, China). The mice were housed in a specific pathogen-free animal facility of Shanghai Jiao Tong University School of Medicine. All mouse experiments were performed under protocols approved by the Institutional Animal Care and Use Committee of the Institute of Health Sciences, Shanghai Institutes for Biological Sciences, and Shanghai Jiao Tong University School of Medicine.

Isolation of mesenchymal stem cells from mouse bone marrow. Bone marrow cells from the bone cavity of femurs and tibias of mice were flushed out with 10% fetal bovine serum (FBS; Hyclone, Logan, UT, USA) in DMEM. All bone marrow cells were passed through a 70 μm cell strainer (BD Bioscience, San Jose, CA, USA) to obtain a single-cell suspension of all nucleated cells. All the single cells were cultured in growth medium (DMEM containing 20% FBS and 1% penicillin-streptomycin (all from Hyclone)) at 37 °C in the presence of 5% CO_2. Non-adherent cells were removed by washing the cultures with PBS twice and replacing the medium after 2 days. The attached cells were cultured and used for experiments at passage 3. Flow-cytometric analysis was conducted to confirm the characteristics of the mesenchymal stem cells. These bone marrow-derived MSCs were positive for CD44 and Sca-1 and negative for CD11b, CD11c, CD34, and CD45.

Ectopic bone formation assay. Approximately 3.0×10^6 of BMMSCs were mixed with β-TCP ceramic particles (45 mg, Shanghai Bio-lu Biomaterials Co., Ltd, Shanghai, China). This mixture was subcutaneously implanted into the dorsal

surface of nude mice, C57BL/6J mice, or B6.129S1-*Il12b*^{tm1Jm}/J mice that were 8–9 weeks old.

To clarify the roles of IL-12 and IL-23 in bone formation *in vivo*, we used 250 μl of HyStem-HP Hydrogel (Hyclone) containing 200 ng IL-12 and 200 ng IL-23 (both from Peprotech, Rocky Hill, NJ, USA) for sustained release. The hydrogel was covered on the surface of the implants in the nude mice. After 8 weeks, the implants were harvested and fixed in 4% paraformaldehyde, then decalcified with 12.5% EDTA (pH 7.0), and then embedded in paraffin. For histological analyses, the sections (5 μm) were stained with hematoxylin and eosin (H&E) and analyzed using ImageJ software (Version 1.49v; NIH, Bethesda, MD, USA). Immunohistochemistry was performed using standard protocols with the antibody: type I collagen (Millipore, Darmstadt, Germany), cleaved caspase 3 (Abcam, Cambridge, MA, USA), and TdT-mediated UTP nick end labeling (Roche Applied Science, Mannheim, Germany). We analyzed the integral optical density (IOD) by using the Image-Pro Plus 6.0 software (Media Cybernetics Inc., Silver Springs, MD, USA) to quantify type I collagen-positive staining.

Cytokine expression in implants. The implants were harvested at five time points, placed in a mortar, and then mixed with 200 μl of lysis buffer. The implants were ground and centrifuged at 12 000 r.p.m. for 10 min. After centrifugation, the supernatant was collected carefully. The cytokine levels in the implants were measured through ProcartaPlex Multiplex Immunoassays (eBioscience, San Diego, CA, USA).

Micro-CT and bone histomorphometry. For micro-CT analysis, the left femurs of both C57BL/6J and B6.129S1-*Il12b*^{tm1Jm}/J mice ($n=5$) were fixed in 4% paraformaldehyde and then scanned with Scanco Medical CT-40 instruments (Scanco Medical AG, Bruttisellen, Switzerland). For histological analyses, the tibias from both C57BL/6J and B6.129S1-*Il12b*^{tm1Jm}/J mice were fixed in 4% paraformaldehyde, decalcified with 12.5% EDTA (pH 7.0), and then embedded in paraffin. After decalcification, the sections (5 μm) were stained with H&E and then analyzed by ImageJ software. Alkaline phosphatase staining was determined using the BCIP/NBT Alkaline Phosphatase Color Development Kit (Beyotime Co., Jiangsu, China) in accordance with the manufacturer's instructions. TRAP staining was determined with a TRAP kit (Sigma-Aldrich, St. Louis, MO, USA) in accordance with the manufacturer's instructions.

Double calcein labeling was performed by intraperitoneal injection of calcein (10 μg/g body weight; C0875; Sigma-Aldrich) at 10 and 3 days before euthanasia. Bones were harvested and embedded in LR white acrylic resin. Serial sections were then cut and imaged using fluorescence microscopy. The MAR (MAR = interlabel width/labeling period) was calculated.

Osteogenic differentiation assay. BMMSCs were cultured in osteogenic medium containing 100 nM dexamethasone, 50 μM ascorbic acid, and 10 mM β-glycerophosphate (all from Sigma-Aldrich). Different doses of IL-12, IL-17, IL-23, and INF-γ (all from Peprotech, Rocky Hill, NJ, USA) were added. To inhibit apoptosis, a pan-caspase inhibitor (Z-VAD-FMK, 20 μM) and a caspase 3 inhibitor (Z-DEVD-FMK, 20 μM, both from Selleckchem, Houston, TX, USA) were used to treat BMMSCs at 4 h before IFN-γ and IL-17 were added. SiRNA for Fas and TRAIL was transfected using Lipofectamine 2000 (Invitrogen, Carlsbad, CA, USA) as described by the manufacturer. The target sequence of Fas mRNA was 5′-CCC GAGAAUUGCUGAAGACAU-3′, that of TRAIL mRNA was 5′-UCUCGGAAAGG GCAUUCAUUU-3′, and that of scramble siRNA (control) was 5′-UUCUCCGAACG UGUCACGU-3′. The medium was changed every 3 or 4 days. To assess osteogenic differentiation, these cultures were stained with Alizarin Red S (Sigma-Aldrich). Finally, the calcium precipitates were dissolved in 0.1 N sodium hydroxide and quantified using a Tecan Safire^2 microplate reader (Tecan, Durham, NC, USA) by absorbance at 548 nm.

CD4+ T-cell isolation and stimulation. Whole spleen from C57BL/6J mouse was extracted and placed in PBS on ice. Splenocytes were obtained by gently grinding the spleen through a 70 μm filter and centrifuging at 300 × *g* for 10 min. Erythrocytes were lysed with RBC lysis buffer, and CD4+ T cells were isolated from the splenocytes using a mouse CD4+ T cell isolation kit (Miltenyi Biotec, Bergisch Gladbach, Germany) in accordance with the manufacturer's instructions. CD4+ T cells were resuspended in culture medium (RPMI-1640 containing 10% FBS and 1% penicillin-streptomycin (all from Hyclone)) at a concentration of 2×10^6/ml. These cells were seeded into 24-well plates precoated with 5 μg/ml anti-CD3 antibody and 2 μg/ml soluble anti-CD28 antibody. IL-12 (10 ng/ml) or IL-23 (25 ng/ml) was also added to the culture medium. Supernatants were collected after 3 days of stimulation and combined with the osteogenic medium to stimulate BMMSCs. CD4+ T cells were then harvested for RNA extraction.

RNA isolation and RT-PCR. Total RNA was isolated using Trizol reagent (Invitrogen, Mulgrave, Australia). The RNA was reverse transcribed into cDNA using the RevertAid Reverse Transcriptase (EP0442; Thermo Scientific, Waltham, MA, USA) in accordance with the manufacturer's instructions. After the reverse transcription reaction, RT-PCR was performed by ViiA 7 Real-Time PCR System (Life Technologies, Gaithersburg, MD, USA) by using SYBR Premix Ex Taq (Takara, Dalian, China) in accordance with the manufacturer's instructions. Experiments were performed in triplicate.

Western blot analysis. Western blot analysis was performed as previously described.[38] In brief, cells were ruptured with ice-cold lysis buffer (50 mM Tris-HCl, pH 7.4, 150 mM NaCl, 1% NP-40, and 0.1% sodium dodecyl sulfate) supplemented with protease inhibitors (Millipore). Cell extracts were centrifuged at 12 000 r.p.m. for 10 min, and the supernatants were collected. Protein samples were resolved by SDS-PAGE and transferred onto PVDF membranes (Millipore). The membranes were blocked in 5% BSA and Tris-buffered saline containing 0.1% Tween-20 for 1 h and then incubated overnight at 4 °C with primary antibodies against ALP (1:500, Santa Cruz, CA, USA), Osx (1:1000, Abcam), OCN (1:500, Santa Cruz), p65, phospho-p65, p38, phospho-p38, JNK, phospho-JNK, Stat1, phospho-Stat1, Caspase 3, Cleaved Caspase 3, Caspase 8, Cleaved Caspase 8 (1:1000, all from Cell Signaling Technology, Danvers, MA, USA), and GAPDH (1:5000, Kangcheng, Shanghai, China). HRP-conjugated secondary antibodies were used at a 1:7500 dilution. The bound antibodies were visualized using the enhanced chemiluminescence detection system (Millipore).

ELISA. The concentrations of serum OCN and CTX-1 in 2-month-old mice were measured using the ELISA kit (Elabscience Biotechnology Co., Ltd, Wuhan, China) in accordance with the manufacturer's instructions. BMMSCs mixed with β-TCP were subcutaneously implanted into the dorsal surface of C57BL/6J mice or B6.129S1-*Il12b*^{tm1Jm}/J mice that were 8–9 weeks old. After 7 days, the mice were killed. Serum was collected from the peripheral blood of C57BL/6J or B6.129S1-*Il12b*^{tm1Jm}/J mice. The serum concentrations of IFN-γ and IL-17 were measured using the ELISA kit (MultiSciences Biotech Co., Ltd, Hangzhou, China) in accordance with the manufacturer's instructions.

Cell survival assay. A Cell Counting Kit-8 (CCK-8; Beyotime Co.) was used to measure the viability of BMMSCs. BMMSCs (1.5×10^4 cells) were seeded in 96-well plates for 24 h and then treated with IL-17 and IFN-γ over a range of concentrations (0 [control], 10, 20, 50, 100, 200 ng/ml). After 6 days, the BMMSCs were assessed using CCK-8 in accordance with the manufacturer's instructions. The absorbance was determined by a Tecan Safire^{2TM} microplate reader (Tecan) at 450 nm. Cell viability was expressed as a percentage of the control (untreated) cells. The cells were stained with 2% toluidine blue O and 2% paraformaldehyde.

TUNEL assay. BMMSCs (5×10^4 cells) were seeded on glass coverslips in 12-well plates and then treated with IL-17 (200 ng/ml) and/or IFN-γ (200 ng/ml) for 4 days. TUNEL assay was performed using the one-step TUNEL kit (Beyotime Co.) in accordance with the manufacturer's instructions. The Cy3-labeled TUNEL-positive cells were imaged under a fluorescent microscope.

Statistical analysis. Statistical significance was assessed using two-tailed Student's *t*-test or analysis of variance (ANOVA). Statistical significance was considered at $P<0.05$. Data are presented as the mean ± S.D.

Conflict of Interest

The authors declare no conflict of interest.

Acknowledgements. This work was supported by grants from National Natural Science Foundation of China (Nos. 81190133, 81401844, 81572123), Science and Technology Commission of Shanghai (Nos. 14431900900, 14140903700, 15411951100), Shanghai Municipal Commission of Health and Family Planning (No.

2013ZYJB0501), and key discipline construction fund of Shanghai education commission (J50206).

1. Kovach TK, Dighe AS, Lobo PI, Cui QJ. Interactions between MSCs and immune cells: implications for bone healing. *J Immunol Res* 2015; **2015**: 752510.
2. Bianco P, Cao X, Frenette PS, Mao JJ, Robey PG, Simmons PJ *et al.* The meaning, the sense and the significance: translating the science of mesenchymal stem cells into medicine. *Nat Med* 2013; **19**: 35–42.
3. Ohishi M, Schipani E. Bone marrow mesenchymal stem cells. *J Cell Biochem* 2010; **109**: 277–282.
4. Ceredig R. A look at the interface between mesenchymal stromal cells and the immune system. *Immunol Cell Biol* 2013; **91**: 3–4.
5. Wei X, Yang X, Han ZP, Qu FF, Shao L, Shi YF. Mesenchymal stem cells: a new trend for cell therapy. *Acta Pharmacol Sin* 2013; **34**: 747–754.
6. Hadjiargyrou M, O'Keefe RJ. The convergence of fracture repair and stem cells: interplay of genes, aging, environmental factors and disease. *J Bone Miner Res* 2014; **29**: 2307–2322.
7. Antonova E, Le TK, Burge R, Mershon J. Tibia shaft fractures: costly burden of nonunions. *BMC Musculoskelet Disord* 2013; **14**: 42.
8. Recknagel S, Bindl R, Brochhausen C, Gockelmann M, Wehner T, Schoengraf P *et al.* Systemic inflammation induced by a thoracic trauma alters the cellular composition of the early fracture callus. *J Trauma Acute Care* 2013; **74**: 531–537.
9. Liu Y, Wang S, Shi S. The role of recipient T cells in mesenchymal stem cell-based tissue regeneration. *Int J Biochem Cell Biol* 2012; **44**: 2044–2050.
10. Pape HC, Marcucio R, Humphrey C, Colnot C, Knobe M, Harvey EJ. Trauma-induced inflammation and fracture healing. *J Orthop Trauma* 2010; **24**: 522–525.
11. Bastian O, Pillay J, Alblas J, Leenen L, Koenderman L, Blokhuis T. Systemic inflammation and fracture healing. *J Leukoc Biol* 2011; **89**: 669–673.
12. Lacey DC, Simmons PJ, Graves SE, Hamilton JA. Proinflammatory cytokines inhibit osteogenic differentiation from stem cells: implications for bone repair during inflammation. *Osteoarthritis Cartilage* 2009; **17**: 735–742.
13. Liu Y, Wang L, Kikuiri T, Akiyama K, Chen C, Xu X *et al.* Mesenchymal stem cell-based tissue regeneration is governed by recipient T lymphocytes via IFN-gamma and TNF-alpha. *Nat Med* 2011; **17**: 1594–1601.
14. Deshpande S, James AW, Blough J, Donneys A, Wang SC, Cederna PS *et al.* Reconciling the effects of inflammatory cytokines on mesenchymal cell osteogenic differentiation. *J Surg Res* 2013; **185**: 278–285.
15. Chang J, Liu F, Lee M, Wu B, Ting K, Zara JN *et al.* NF-kappaB inhibits osteogenic differentiation of mesenchymal stem cells by promoting beta-catenin degradation. *Proc Natl Acad Sci USA* 2013; **110**: 9469–9474.
16. Djouad F, Bouffi C, Ghannam S, Noel D, Jorgensen C. Mesenchymal stem cells: innovative therapeutic tools for rheumatic diseases. *Nat Rev Rheumatol* 2009; **5**: 392–399.
17. Franz S, Rammelt S, Scharnweber D, Simon JC. Immune responses to implants – A review of the implications for the design of immunomodulatory biomaterials. *Biomaterials* 2011; **32**: 6692–6709.
18. Claes L, Recknagel S, Ignatius A. Fracture healing under healthy and inflammatory conditions. *Nat Rev Rheumatol* 2012; **8**: 133–143.
19. Konnecke I, Serra A, El Khassawna T, Schlundt C, Schell H, Hauser *et al.* T and B cells participate in bone repair by infiltrating the fracture callus in a two-wave fashion. *Bone* 2014; **64**: 155–165.
20. Vignali DAA, Kuchroo VK. IL-12 family cytokines: immunological playmakers. *Nat Immunol* 2012; **13**: 722–728.
21. Trinchieri G, Pflanz S, Kastelein RA. The IL-12 family of heterodimeric cytokines: new players in the regulation of T cell responses. *Immunity* 2003; **19**: 641–644.
22. Okamoto S, Fujiwara H, Nishimori H, Matsuoka K, Fujii N, Kondo E *et al.* Anti-IL-12/23 p40 antibody attenuates experimental chronic graft-versus-host disease via suppression of IFN-gamma/IL-17-producing cells. *J Immunol* 2015; **194**: 1357–1363.
23. Lange T, Schilling AF, Peters F, Haag F, Morlock MM, Rueger JM *et al.* Proinflammatory and osteoclastogenic effects of beta-tricalciumphosphate and hydroxyapatite particles on human mononuclear cells *in vitro*. *Biomaterials* 2009; **30**: 5312–5318.
24. Janicki P, Kasten P, Kleinschmidt K, Luginbuehl R, Richter W. Chondrogenic pre-induction of human mesenchymal stem cells on β-TCP: Enhanced bone quality by endochondral heterotopic bone formation. *Acta Biomater* 2010; **6**: 3292–3301.
25. Wang RX, Yu CR, Mahdi RM, Egwuagu CE. Novel IL27p28/IL12p40 cytokine suppressed experimental autoimmune uveitis by inhibiting autoreactive Th1/Th17 cells and promoting expansion of regulatory T cells. *J Biol Chem* 2012; **287**: 36012–36021.
26. Zhang Y, Li X, Chihara T, Mizoguchi T, Hori A, Udagawa N *et al.* Comparing immunocompetent and immunodeficient mice as animal models for bone tissue engineering. *Oral Dis* 2015; **21**: 583–592.
27. Hunter CA. New IL-12-family members: IL-23 and IL-27, cytokines with divergent functions. *Nat Rev Immunol* 2005; **5**: 521–531.
28. Dong C. Diversification of T-helper-cell lineages: finding the family root of IL-17-producing cells. *Nat Rev Immunol* 2006; **6**: 329–333.
29. Vilisaar J, Kawabe K, Braitch M, Aram J, Furtun Y, Fahey AJ *et al.* Reciprocal regulation of substance P and IL-12/IL-23 and the associated cytokines, IFNgamma/IL-17: a perspective on the relevance of this interaction to multiple sclerosis. *J Neuroimmune Pharmacol* 2015; **10**: 457–467.
30. Rebane A, Zimmermann M, Aab A, Baurecht H, Koreck A, Karelson M *et al.* Mechanisms of IFN-gamma-induced apoptosis of human skin keratinocytes in patients with atopic dermatitis. *J Allergy Clin Immunol* 2012; **129**: 1297–1306.
31. Viard-Leveugle I, Gaide O, Jankovic D, Feldmeyer L, Kerl K, Pickard C *et al.* TNF-alpha and IFN-gamma are potential inducers of Fas-mediated keratinocyte apoptosis through activation of inducible nitric oxide synthase in toxic epidermal necrolysis. *J Invest Dermatol* 2013; **133**: 489–498.
32. Rakshit S, Chandrasekar BS, Saha B, Victor ES, Majumdar S, Nandi D. Interferon-gamma induced cell death: Regulation and contributions of nitric oxide, cJun N-terminal kinase, reactive oxygen species and peroxynitrite. *Biochim Biophys Acta* 2014; **1843**: 2645–2661.
33. Refaeli Y, Van Parijs L, Alexander SI, Abbas AK. Interferon gamma is required for activation-induced death of T lymphocytes. *J Exp Med* 2002; **196**: 999–1005.
34. Badie B, Schartner J, Vorpahl J, Preston K. Interferon-gamma induces apoptosis and augments the expression of Fas and Fas ligand by microglia in vitro. *Exp Neurol* 2000; **162**: 290–296.
35. Langaas V, Shahzidi S, Johnsen JI, Smedsrod B, Sveinbjornsson B. Interferon-gamma modulates TRAIL-mediated apoptosis in human colon carcinoma cells. *Anticancer Res* 2001; **21**: 3733–3738.
36. Abadie A, Wietzerbin J. Involvement of TNF-related apoptosis-inducing ligand (TRAIL) induction in interferon gamma-mediated apoptosis in Ewing tumor cells. *Ann NY Acad Sci* 2003; **1010**: 117–120.
37. Teng MW, Bowman EP, McElwee JJ, Smyth MJ, Casanova JL, Cooper AM *et al.* IL-12 and IL-23 cytokines: from discovery to targeted therapies for immune-mediated inflammatory diseases. *Nat Med* 2015; **21**: 719–729.
38. Li J, Zhang N, Huang X, Xu J, Fernandes JC, Dai K *et al.* Dexamethasone shifts bone marrow stromal cells from osteoblasts to adipocytes by C/EBPalpha promoter methylation. *Cell Death Dis* 2013; **4**: e832.

Supplementary Information accompanies this paper on Cell Death and Differentiation website (http://www.nature.com/cdd)